Force Measurements Between a Bacterium and Another Surface *In Situ*

RUCHIREJ YONGSUNTHON AND STEVEN K. LOWER
Ohio State University, Columbus, Ohio 43210

I. Introduction

In most natural environments, including the human body, bacteria live on surfaces where they create an interface between themselves and an inert or living substrate (Parsek and Fuqua, 2004; Watnick and Kolter, 2000; Whitman *et al.*, 1998). Figure 1 (see color insert) presents images of gram-negative and gram-positive bacteria on an inorganic surface. Images such as these provide a visual depiction of a bacterium in contact with another surface. However, the actual bacterium-substrate interface is hidden from view. One would need to be able to peer under the bacterium to reveal the intrinsic forces and surface-sensing mechanisms that govern the formation of an interface between a cell and another surface. In other words, it is what we cannot see that dictates whether an interface is created between a bacterium and a substrate.

Fundamental forces such as van der Waals, electrostatic, solvation, and steric interactions (Table I) are expected to control the way in which a bacterium's cell wall physically interacts with another surface. It has traditionally been very difficult to probe these forces because of the small magnitude and length scale over which they operate. Over the last several years, we have developed and refined an atomic force

ADVANCES IN APPLIED MICROBIOLOGY, VOLUME 58
0065-2164/06 $35.00
DOI: 10.1016/S0065-2164(06)58003-1

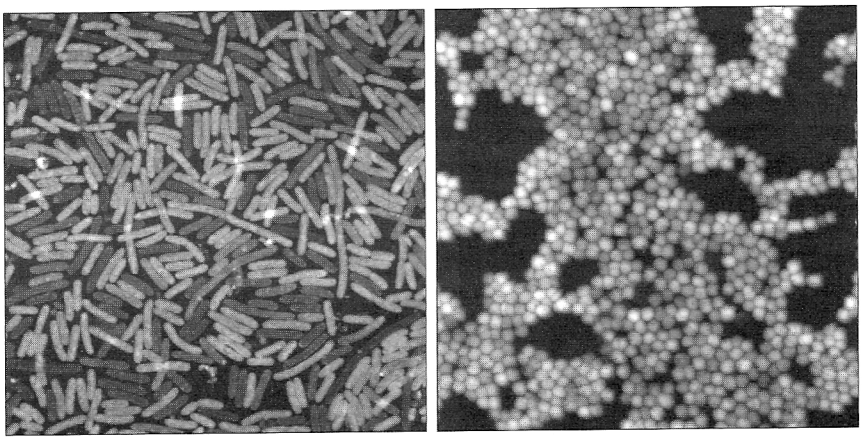

FIG. 1. Atomic force micrographs. (Left) Gram negative bacteria (*Shewanella*) on a glass substrate; scale = 40 μm × 40 μm. (Right) Gram-positive bacteria (*Staphylococcus*) on a glass substrate; scale 25 μm × 25 μm.

TABLE I

SUMMARY OF FORCES AT THE BACTERIUM-(BIO)MATERIAL INTERFACE*

Type of interaction	Description (attractive/repulsive & range of operation)
Nonspecific	
van der Waals	Force due to polarization of adjacent particles; usually attractive; length scale is typically a few nm
Electrostatic	Force between charged particles; attractive for particles of opposite sign; repulsive for particles of similar sign; length scale is 1–100 nm depending upon the ionic strength of the solution
Solvation	Hydration force is typically repulsive due to sorbed water layers; length scale is approximately the size of a water layer(s)
	Hydrophobic force is attractive between nonpolar surfaces; length scale is on the order of tens of nm to less than 100 nm
Steric	Repulsive force associated with the entropic confinement of polymers; range may be tens of nm
Specific	Attractive force or bond between a ligand and its complementary receptor; specific forces result because of unique combinations of several different types of nonspecific forces

* This classification follows that of Israelachvili, 1992; Israelachvili and McGuiggan, 1988; Leckband and Israelachvili, 2001.

microscopy (AFM) (Binnig *et al.*, 1986) technology that allows the controlled creation of a bacterium-substrate interface and the concurrent measurement of forces that operate within this interface (Lower *et al.*, 2000, 2001b). This article will provide an overview of how to use AFM to measure forces between a living bacterium and an inanimate surface (or another cell). This review is not intended to serve as an authoritative text on all force studies that have been conducted with AFM. For this, the reader is referred to other publications (e.g., Butt *et al.*, 1995; Cappella and Dietler, 1999; Kendall and Lower, 2004). Rather, this report is meant to provide practical advice on using AFM to physically probe forces between bacteria and the surfaces upon which they make contact.

AFM is a scanning probe microscopy technique that provides information about a localized portion of a sample by sensing the behavior of a small tip-cantilever system, which interacts with the sample (Fig. 2). For example, the topography on a sample, as shown in Fig. 1, may be

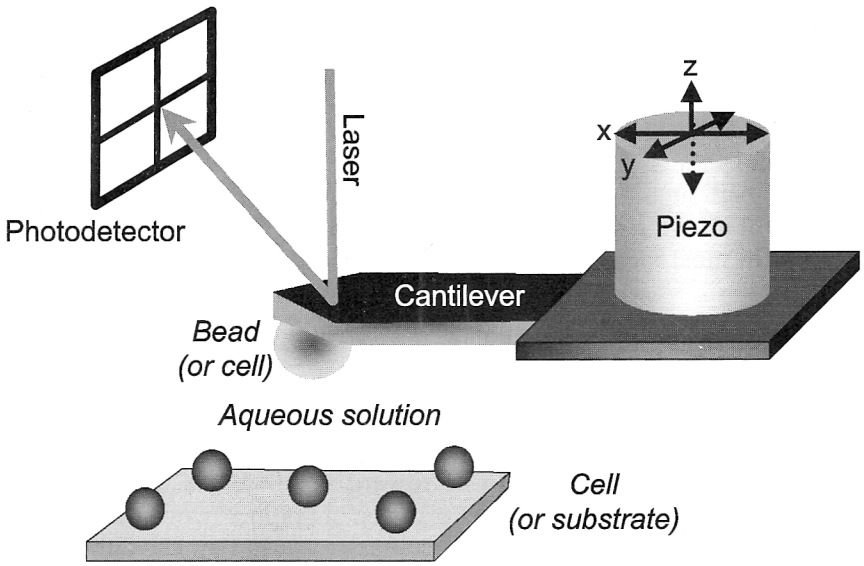

FIG. 2. Schematic of the key components of an atomic force microscope (AFM). The piezoelectric scanner translates the AFM probe laterally (x, y) and/or vertically (z) relative to the sample (cell or substrate). Forces between the "free end" of the probe and the sample are transduced into deflection of the cantilever. The behavior of the cantilever is monitored by tracking a laser beam reflected off the top side of the cantilever and onto a photodetector. Forces between a bacterium and another surface can be directly measured by functionalizing the AFM probe with a colloidal bead or living cell and scanning the piezo in only the z dimension.

determined by monitoring the deflection of the cantilever as the tip is scanned across the sample, much in the same way that a person reads Braille by sweeping fingers across a page. Although AFM can provide an image of a sample, it should not be confused with optical microscopy, which uses light to directly probe the sample rather than a tip-cantilever probe. By turning off the lateral scanning mechanism, the cantilever tip can be made to move toward and away from a specific point on a specimen. Attractive or repulsive forces between the tip and the sample will cause the cantilever to bend downward or upward. Under reasonable perturbation, the cantilever behaves like a spring such that force (F in N) is given by Hook's Law $F = -(K_{sp})(x)$, where K_{sp} is the cantilever spring constant (N m^{-1}) and x is the deflection of the lever (in m). Hence, AFM can be used to quantitatively measure atomic and molecular forces between a probe and a specimen in real time and in aqueous solution.

II. Components of an AFM

The key components of an atomic force microscope include: a force-transducing cantilever, a piezoelectric scanner to translate the cantilever toward and across a sample (or, in some instruments, the scanner moves the sample relative to the cantilever), and a laser and photodiode detector system, which tracks the behavior of the cantilever (Fig. 2). Although most AFM usage (e.g., topographic imaging) requires the use of all three axes of scanner movement, only the vertical (z) axis is used in most force measurements.

A. Force-Transducing (or Sensing) Cantilever

Commercially available force-transducing cantilevers may be V-shaped silicon nitride levers or single beam silicon levers (Albrecht *et al.*, 1990; Tortonese, 1997). The longer and thinner a cantilever, the more sensitive it will tend to be toward small forces. However, the sensitivity typically comes at the expense of responsiveness and lateral stability, so cantilevers must be specifically chosen for the application at hand. When obtaining cantilevers for force measurements, perhaps the most important property to consider is the cantilever's spring constant. The spring constant of single beam (or "diving board") silicon cantilevers is on the order of tens of N m^{-1}. These cantilevers are often too stiff to detect the small forces between a cell (or biomolecule) and a material surface. V-shaped silicon nitride cantilevers have nominal spring constants from 0.58 to 0.01 N m^{-1}. Because of their sensitivity

and greater lateral stability, V-shaped cantilevers are typically used for force measurements between biological and material surfaces.

It is important to note that the nominal spring constant of a cantilever can vary significantly from the actual value (Senden and Ducker, 1994). There are a number of methods for calibration of the cantilever spring constant. Perhaps those best suited to biological force measurements are the Cleveland method (Cleveland *et al.*, 1993) and the hydrodynamic drag method of Craig and Neto (Craig and Neto, 2001). The former method requires increasing the mass of the tip by known amounts and measuring the resulting shift in resonance frequency. The addition of mass is accomplished by attaching tungsten beads to the end of a cantilever (see the following discussion on how to attach a bead to a cantilever). Increasing mass causes a cantilever's resonance frequency to decrease, and the resonance peak will become more distinct (i.e., sharper). Plotting mass vs the squared inverse resonance frequency (in rad s^{-1}) of a cantilever results in a linear relationship with a slope equal to the spring constant of the cantilever (Cleveland *et al.*, 1993). The Cleveland method is popular because it is easy to use and is effective for obtaining averages for cantilevers manufactured from the same wafer. However, this method is not as well suited for calibration of a single probe.

The Craig and Neto hydrodynamic method (Craig and Neto, 2001) involves measuring the cantilever deflection caused by viscous drag on a colloidal probe (i.e., cantilever supporting a small bead) as the probe approaches a flat surface at varying speeds. For small colloids and surface separations and low Reynolds numbers, Brenner's relation for the hydrodynamic drag force on a colloid can be approximated by $F = 6\pi\eta r^2 U/z$, where η is the fluid viscosity (typically in Pa s), r is the radius of the colloidal sphere (in m), U is the velocity with which the sphere approaches the surface (in m s^{-1}), and z is the distance between the surface of the sphere and the flat surface (in m). The cantilever deflection $F = kx = 6\pi\eta r^2 U/z$ allows extraction of the spring constant. (e.g., plotting the cantilever deflection x versus $1/z$ will yield a linear relation with slope $6\pi\eta r^2 U/k$). Although the Craig and Neto method requires the use of a rather viscous fluid with known viscosity (e.g., sucrose solutions), it is relatively nondestructive, it can be performed on a single AFM cantilever, and it is particularly well suited to experiments that require a colloidal probe.

For the sake of completeness, we should mention that various other methods of cantilever calibration exist and may sometimes be better suited for a particular application. For example, a cantilever of interest can be pressed against a standard cantilever with a known spring

constant. These force calibration cantilevers are available commercially (e.g., from Veeco-Digital Instruments), but they are only valid for cantilevers with a spring constant >0.1 N m^{-1}. Other methods for determining a spring constant include measuring the resonant frequency of a cantilever when it oscillates due to thermal vibrations (Hutter and Bechhoefer, 1993).

While it is desirable to measure the spring constant of every cantilever used in an experiment, this is not always convenient or even possible. The Craig and Neto method does allow for calibration of a single probe but is not optimally accurate for determining the "as-is" bare cantilever stiffness. The Cleveland method requires that fairly heavy (e.g., tungsten) beads be glued to the end of a cantilever, thereby rendering the cantilevers useless for force measurements. Fortunately, commercial manufacturing practices are very reproducible, so that cantilevers from the same batch have spring constants within 10% of the average value (Senden and Ducker, 1994). Therefore, a few cantilevers from a given batch can be sacrificed to determine an average spring constant for a particular cantilever (e.g., long, narrow, V-shaped silicon nitride cantilever) from a given batch. As a check, one should measure the resonant frequency, which is directly related to intrinsic properties of a cantilever, for every cantilever from a given batch to verify consistency.

When determining relative forces with a single cantilever, calibration is not required. However, to compare values between different cantilevers or with other published values, a calibration of the cantilever spring constant is necessary. Many AFM users will rely on the spring constant values quoted on their box of tips. While these quoted values may be used for rough comparisons, the resulting values are not sufficiently reliable for published data of absolute forces.

B. Piezoelectric Scanner

The piezoelectric scanner that moves the AFM cantilever relative to the sample, or vice versa, depending on the AFM configuration, is the source of all resulting dimensional information. A piezoelectric material contracts and expands proportionally to an applied voltage. Voltages applied along three (ideally) orthogonal axes (x, y, z) allow control of the tip and sample separation (see Fig. 2). The scanner sensitivity is a measure of how the piezo responds to applied voltage and is commonly expressed as the ratio of piezo movement (nm) to applied voltage (V), specified for each scanner axis. The conversion from applied voltage to actual dimensional information is generally

performed by the AFM data acquisition software and thus is often taken for granted by the user. However, there are some common sources of piezo inaccuracy that can lead to misleading dimensional information in force measurements.

The most important and most overlooked source of error is due to changes in the piezo sensitivity (applied voltage per nm of piezo displacement, usually specified for each scanner axis), which generally decreases exponentially with time of usage. However, under heavy use, the scanner sensitivity can decrease more dramatically. For example, sensitivity of the *z*-axis piezo (perpendicular to the sample plane) in one of our scanners decreased by 18% during the first year of use, and then an additional 22% after 6 months of heavy use. The piezo sensitivity also varies with the size of the scan; a scanner calibrated for accurate operation in one range may be inaccurate in a different range. Many AFM users forget this and tend to interpret the distance data as "truth" (100% accurate). However, the distances reported by the software are only as accurate as allowed by the quality of the scanner calibration.

AFM users should routinely check the reliability of the "applied volts to nm" piezo conversion by looking at a known standard. Most data acquisition software has a calibration option where a standard with known dimensions is measured and sensitivity parameters are adjusted until the spatial dimensions fall within tolerance. Even if a "perfect" calibration has been performed, it is unlikely to hold indefinitely, especially if the scanner is frequently used to its extremes (maximum extension and compression), as is common in force measurements. In our experience, the *z*-axis sensitivity changes more dramatically than the *x*- and *y*-axes (parallel to the sample plane; see Fig. 2). If a "perfect" calibration was performed recently, AFM users should still check for validity of piezo calibration in their range of interest, because sensitivity may change with scan size. When collecting force curves in a length range significantly different than that of the calibration standard, the original calibration may not hold. For example, if a 50 nm height calibration standard is used, the resulting sensitivities are unlikely to be accurate for operation in the 1 μm range for the *z*-axis scanner.

The best way to insure accurate interpretation of the data is to perform a general calibration with a reference standard of reasonable dimensions and then determine a correction factor for the specific range of interest. The correction factor can be found by measuring a standard and determining the ratio between the "true" standard size and the measured size. For example, our *z*-piezoelectric scanner was

recently calibrated for accuracy in the 25–100nm range using two National Institute of Standards and Technology-(NIST) certified calibration gratings (MikroMasch, Portland, OR): TGZ01C (26.4 ± 0.6nm, traceable to NIST 821/261141–99) and TGZ02C (102.3nm ± 1.4nm, traceable to NIST 821/261141–99). These standards are composed of one-dimensional arrays, of rectangular SiO_2 steps on a Si wafer. Standards TGZ01C and TGZ02C were measured to be 31.3 ± 0.3nm and 120.2 ± 0.8nm, respectively. Averaging the correction factors obtained from these two measurements and propagation of errors yields a divisional correction factor of 1.18 ± 0.02nm. All raw piezo scanner displacement values were corrected, yielding results with 2% uncertainty (the uncertainty in *z*-piezo linearity).

C. Laser and Photodiode Detector System

In commercial AFMs, the behavior of the cantilever is monitored by tracking the reflection of a laser beam off the top of the cantilever and onto a photodiode-based detector (Fig. 2). The optical path between the cantilever and photodetector system is long enough (at least several centimeters) so that even nanoscale deflections of the cantilever result in measurable shifts in the position of the laser spot on the photodetector. Optimal accuracy of the cantilever detection requires that the laser spot be optimally placed on the cantilever. The spot should be on the distal edge of the free end of the cantilever, but in such a manner that the reflected laser intensity on the detector (called the "sum" in many commercial systems) is high. The spot should also be symmetrically placed on the cantilever by adjusting the position of the laser until the sum is maximized, rather than by visual inspection of the physical laser spot on the cantilever.

III. Force Data

In raw form, AFM force data are measured as the output voltage from a photodiode detector (which is related to cantilever deflection) as a function of applied voltage on the piezoelectric scanner (which is related to tip-sample separation). In order to convert the raw measurements into meaningful physical quantities, the photodiode output voltage must be converted to cantilever deflection and the piezoelectric applied voltage must be converted to distance. The cantilever deflection can then be converted to force values, the accuracy of which depends on the accuracy of both the voltage-distance conversions and the cantilever spring constant.

A. Converting Photodetector Voltage into Force Values

The photodiode output signal, which is related to the position of the reflected laser spot (Fig. 2), is measured in volts. These voltages correspond to the upward or downward movement of the free end of the cantilever in response to repulsive or attractive forces between the tip and sample. Detector voltage measurements must be converted into force values using the spring constant of the cantilever (N m^{-1}) and a "volts to nm" conversion factor. This photodiode conversion is called the "optical lever sensitivity" (in nm V^{-1}), and should not be confused with the "volts to nm" conversion (piezo sensitivity) used to translate the applied scanner voltage into scanner displacement (as previously noted). The optical lever sensitivity allows the signal from the photodiode detector (in volts) to be converted into deflection (in nm) values for the cantilever. When the cantilever is pressed into contact with a hard surface, each unit of piezo movement ideally corresponds to an equivalent deflection of the cantilever. The inverse slope of the "region of contact" (also referred to as the "region of constant compliance") is often used to determine the optical lever sensitivity (Fig. 3). For the data shown in Fig. 3, the optical lever sensitivity is ~120 nm V^{-1}. Each voltage value is multiplied by the optical lever sensitivity to determine the upward or downward deflection of the cantilever in response to repulsive or attractive forces, respectively.

One important point to consider is that this conversion is accurate only if the cantilever itself is the most compliant or flexible component of the system. This includes not only the cantilever but also the sample and any cells or biological polymers that may be attached to the cantilever. This criterion may not be met for many soft materials such as biological cells.

It may therefore be necessary to have other means of determining the optical lever sensitivity. One method is to determine the optical lever sensitivity for a cantilever on a hard surface, such as mica or a glass slide, before and after force measurements. Assuming that the optical path and other parameters of an experiment do not change, this may be a valid proxy for determining the optical lever sensitivity. However, this method cannot be used if a cantilever has been functionalized with cells (see following explanation).

In such instances, the "photodiode shift voltage" can be used to determine the optical lever sensitivity (D'Costa and Hoh, 1995; Lower *et al.*, 2001b). The photodiode shift voltage conversion relies on the fact that the optical lever sensitivity depends largely on the shape and position of the laser spot on the detector. Once a correlation between

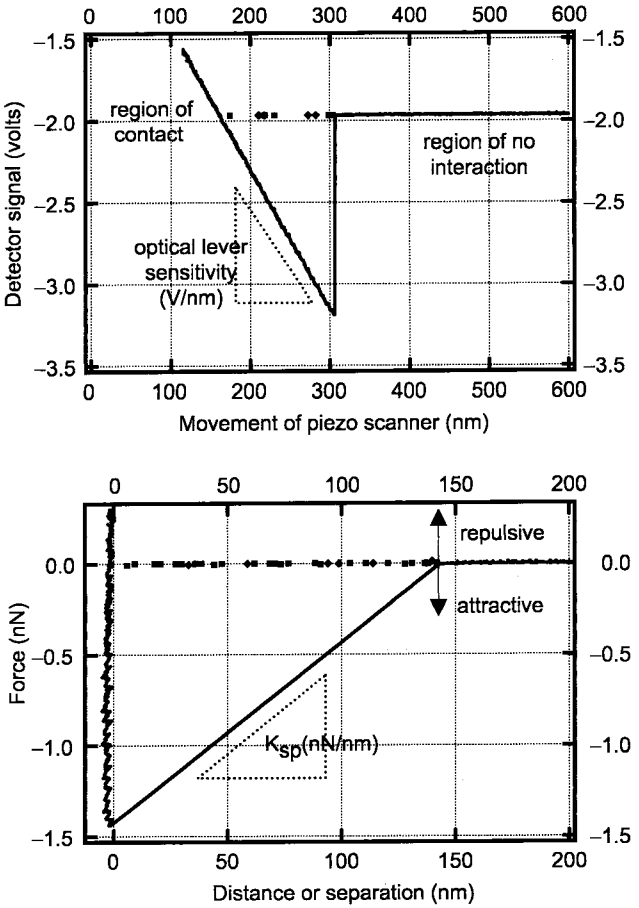

FIG. 3. The approach (dotted) and retraction (solid) force curves for a glue-contaminated AFM tip on a glass substrate in aqueous solution. (Top) The raw voltage output of the photodetector is plotted as a function of the *z*-piezo movement, which has already been converted from the voltage applied to the *z*-piezo scanner. In the region of contact, each unit of piezo movement ideally results in equivalent cantilever deflection (i.e., cantilever deflects 1nm if the piezo moves 1nm). The inverse slope in this region yields the optical lever sensitivity, 120 nm V^{-1}, which is a measure of how the photodetector responds as the cantilever flexes. (Bottom) The force between the tip and sample as a function of the separation between the surfaces of the tip and sample. The photodetector output (top plot) was converted to cantilever deflection (in nm), which in turn was converted to force, assuming a spring constant of 0.01 nN/nm. The piezo movement was corrected to account for deflection of the cantilever and yield the separation between tip and sample. By convention, repulsive forces take a positive sign and attractive forces are negative. So-called "jump-from" or "jump-to" contact features result from the mechanical instability of the cantilever relative to the forces it is probing.

the photodiode shift voltage and optical lever sensitivity is established for a given instrument, it can be used to obtain an accurate measure of optical lever sensitivity without relying on the region of contact. One drawback of the photodiode shift voltage conversion is that it is specific to the scanner, fluid cell, diode laser, and cantilever (e.g., the long, narrow silicon nitride cantilevers sold by a particular vendor). Further, the photodiode shift voltage for a particular experiment must be measured in real time. It is not a property that is stored with a force curve as is the region of contact.

The use of the region of contact (region of constant compliance) to determine optical lever sensitivity will result in an overestimate of forces when the cantilever is not the most compliant component of the system. It will also lead to error in the conversion of piezo movement into separation, which is discussed later in this article. It should be noted that if the region of constant compliance is large enough, the cell might be compressed to the point where the cantilever is more compliant. In this case, the perceived optical level sensitivity, taken from the high compression region, approaches the "true" value. However, the extreme force involved in such cell compressions could damage the cell and/or contaminate the cantilever tip with cell matter.

Once the photodiode signal (V) is converted to a cantilever's deflection (m), the spring constant (N m^{-1}) is used to convert the deflection values into force data (N). The region of no contact is defined as zero force (see Fig. 3). Anything above this line (i.e., positive values) indicates repulsion, whereas any datum point below this line (i.e., negative values) indicates attractive forces between the tip and sample.

B. Converting Movement of the Piezoelectric Scanner into Separation Values

As discussed earlier, the applied voltage to the piezo determines the scanner displacement, which also corresponds to the displacement of the fixed end of the AFM cantilever (see Fig. 2). The movement of the piezoelectric scanner must be corrected by the deflection of the free end of the cantilever to obtain an absolute separation distance between a sample (e.g., a cell attached to a substrate) and the tip on the cantilever.

Jump-from contact features can be seen in retraction curves when the cantilever spring constant exceeds the actual force gradient at the tip-glass interface (see K_{sp} label on bottom figure). Jump-to-contact features may be present in approach data when the actual force gradient exceeds the spring constant of the cantilever (see distance of 0–10 nm in approach curve in the bottom figure).

The separation between the tip and sample can be determined once the photodiode signal is converted into deflection values for the cantilever. This is accomplished by correcting the movement of the piezoelectric scanner by the cantilever deflection to obtain an absolute separation. For example, if the piezoelectric scanner moves the cantilever 10nm toward the sample, but the free end of the cantilever deflects upward by 2 nm, then the actual separation has changed by only 8 nm. See Fig. 3 for an example of the conversion from piezo displacement to separation. The origin of the separation axis (i.e., distance of zero) is defined by using "jump-to-contact" and "jump-from-contact" events for approach and retraction curves, respectively (see Fig. 3). In instances where only repulsive forces are measured (i.e., no jump to/from contact), it is more difficult to define a separation distance of zero. This is typically accomplished by defining the initial point of the region of contact as the origin of the separation axis.

IV. AFM Force Measurements

A. Functionalizing the AFM Probe

The interaction detected by an AFM depends on the nature of the probe used in the force-measuring experiments. Force-sensing cantilevers can be used "as is" to measure forces between a bacterium on a glass cover slip and silicon or silicon nitride tip. However, these two materials are often irrelevant to materials found in environmental or biological systems. Therefore, AFM probes are fabricated or modified with a variety of inorganic or biological particles or substances (Table II).

TABLE II

Some Examples of Substances Used to Functionalize an AFM Probe

Functionalizing substance	Reference
Nucleic acid	Boland and Ratner, 1995; Lee *et al.*, 1994
Protein or antibody	Florin *et al.*, 1994; Hinterdorfer *et al.*, 1996; Lee *et al.*, 1994; Moy *et al.*, 1994a, 1994b; Willemsen *et al.*, 1999
Polysaccharide	Dammer *et al.*, 1995; Frank and Belfort, 1997
Bacteria or fungus cell	Bowen *et al.*, 2000; Lower *et al.*, 2000, 2001a,b, 2005; Razatos *et al.*, 1998
Colloid/bead	Ducker *et al.*, 1991, 1992

Below is a discussion on how to functionalize an AFM probe with a colloidal bead (e.g., glass or latex) or living bacterial cells, either of which can be used to probe forces on cells attached to a cover slip.

1. *Colloid Bead Probe*

There are no fixed recipes for probe functionalization, and unfortunately, a great deal of trial and error is involved, even when working with a "known" recipe. It is often best to begin by cleaning all nonbiological surfaces. New tips from a factory-sealed box are often contaminated by the adhesive used to secure the tip within the box (Lo *et al.*, 1999). Similarly, silica spheres, glass slides, and cover slips often have proprietary coatings to keep them from sticking together. Inorganic materials like the tips, silica spheres, and glass cover slips can all be cleaned by soaking in piranha solution, which is a 1:1 mixture (by volume) of 70% sulfuric acid and 30% hydrogen peroxide. We often clean our tips and glass surfaces by soaking them in piranha solution for several hours, rinsing thoroughly (>10X) in ultrapure water, and drying them under a stream of nitrogen gas. This piranha cleaning solution should be used with extreme care. Protective gloves, goggles, face shield, and clothing must be worn, and the chemicals must be manipulated within a chemical hood.

Attaching a glass (or polystyrene) bead to the end of a cantilever (Fig. 4, see color insert) requires a great deal of patience and practice. It is wise to begin with dry, glass (silica) beads on the order of 10–50 μm (e.g., from Duke Scientific or Polysciences). The beads should be distributed on a clean substrate with sufficient inter-bead spacing so that the AFM tip can easily approach the bead chosen for attachment.

Beads can be attached to the cantilever with various adhesives. An adhesive that is inert in aqueous solution should be used in this procedure. The adhesive should preferably have substantial bulk to fill the gaps between the colloidal sphere and the flat cantilever surface. There are a variety of choices, including 5-minute epoxy, thermal glues, and resins that cure under UV light. Studies have been conducted to determine whether certain adhesins will degas into solution, thereby contaminating an experiment (Pincet *et al.*, 1995). "Crazy glue," which is popular in department stores, should not be used, as it does not fill gaps well, degasses quickly, and does not bond effectively in solution.

In theory, the procedure for bead attachment is very simple: place a small quantity of epoxy on the end of the cantilever and then position a bead on the epoxy. A three-dimensional micromanipulator can be used to accomplish this, but these are often very expensive. An alternative

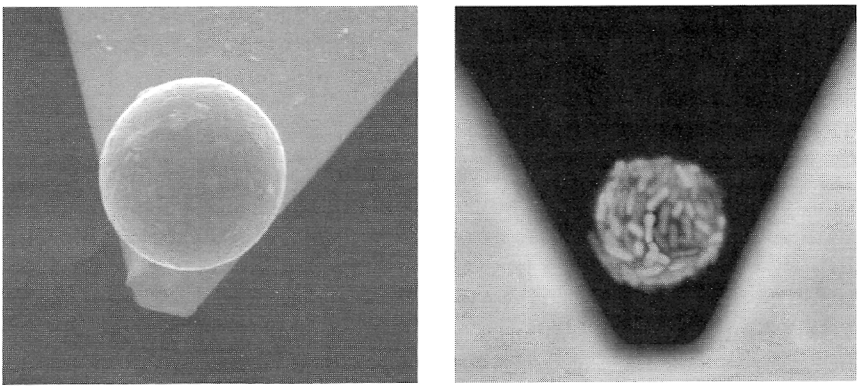

FIG. 4. (Left) Scanning electron micrograph of a colloid probe created by gluing a bead (e.g., glass, shown here, or latex) to the end of a cantilever. (Right) Fluorescence image of a biologically active force probe created by attaching a bacteria-coated bead (or single bacterium, not shown) to a cantilever (modified from Lower *et al.*, 2000). Bacteria cells can be transformed with a plasmid for the green fluorescent protein. Fluorescence from this intracellular protein can be used as a convenient, nondestructive means of observing cells on the probe. Both images show a bead that is ~10 μm in diameter.

method is to use the AFM itself, preferably one that is fitted with an optical microscope with at least 100X magnification (including the magnification of the eyepiece). Great care should be exercised when using epoxy or glue near the piezoelectric scanner of a force microscope. A small (<0.2 mm) drop of epoxy can be placed on a cleaved piece of mica or glass slide. An optical microscope can be used to position the end of the cantilever directly over the edge (not in the middle) of the epoxy. The end of the cantilever should be lowered into the glue until it just makes contact and then quickly removed before too much glue wicks along the cantilever surface. If the tip is moved laterally from the edge of the glue, excess resin will often wick off the tip onto the surface, much like ink wicks off a quill. Excess glue can also be removed by tapping the cantilever onto a clean section of the mica or glass substrate, but aggressive dabbing may damage the cantilever. The substrate supporting the glue should be replaced with another clean substrate that supports the beads. The cantilever should be positioned over a single sphere and lowered until the epoxy on the cantilever touches the sphere. If successful, the bead will be lifted away from the mica or glass substrate as the cantilever is withdrawn.

Successful attachment of a bead onto a cantilever will require a number of trials. New AFM users should not be discouraged by initial

failures. It is best to practice with old cantilevers. Great care should be exercised in centering the bead on the end of a cantilever, as the position of a bead on a cantilever can impact the spring constant of that cantilever (Sader, 1995). Of course, one will also need to ensure that the epoxy does not contaminate the bead surface. This can be accomplished by measuring forces between a glass-bead probe and a glass cover slip (as described below) and comparing those measurements to another probe that has been intentionally contaminated with epoxy. Many epoxies also fluoresce, which is another way to observe potential contamination on a glass bead.

Once fabricated, a colloidal probe can be used in AFM force measurements. Alternatively, the surface of the colloid (e.g., glass bead) can be further modified with biological molecules (see Table II) and then used in an AFM. Next, we will discuss the activation of a colloid probe with living bacterial cells, thereby creating a biologically active force-probe.

2. *Bacteria Probe or Biologically Active Force-Probe*

There may be instances where one wishes to measure forces between two cells or between a bacterium and a specific face of a mineral. This requires the AFM probe to be functionalized, or activated with cells. This is more challenging than linking a glass or latex bead to an AFM probe, but the principle is the same. A bead coated with living cells is attached to the end of a cantilever, creating a so-called biologically-active-force-probe (Fig. 4).

Attachment of a bacteria-coated bead to a cantilever requires a great deal of practice, because the bead must remain hydrated at all times. It is best to practice with bare glass beads in solution (after mastering the attachment of dry beads). With practice, a single bacterium can even be linked to the end of a cantilever (Lower *et al.*, 2001b). Measuring forces with a single bacterium may seem to be a more ideal choice than measuring forces with a bacteria-coated bead. But, the contact area in a force measurement is typically less than the size of one bacterium, even for a bacteria-coated bead. Furthermore, directly attaching a single cell to the cantilever creates a situation in which a very large cantilever surface is placed in close proximity to a relatively small bacterium. The presence of such a large cantilever surface may impact the forces that are detected with the AFM, especially in low-ionic strength solutions where the electrostatic double layer (see the following section) is very large.

Various silane linkers (e.g., aminopropyltriethoxysilane or octadecyltrichlorosilane; see Pleuddemann, 1991) can be used to attach

bacteria to glass surfaces. We will describe one of these procedures in the next section. When selecting a silane linker it is important to consider the relative difference between those forces binding the cells *to* the AFM probe, and the forces that will be probed *by* the cells *on* the probe. A relatively strong force must hold bacteria to the probe; otherwise the cells will be removed from the probe during force measurements. The strength of this bond can be evaluated by simply using a microscope to confirm that cells remain on the AFM probe at all times during force measurements. Silane molecules (or other linkers) can be selected on a case-by-case basis, depending on the bacteria species of interest.

Obviously the linker molecule should not cause the bacteria to die. Cell viability can be assessed by placing a biologically-active-force-probe on an agar plate. Assuming appropriate aseptic techniques are followed, activity of cells is confirmed by the presence of a colony on the agar. Others may wish to use a LIVE/DEAD stain (e.g., from Molecular Probes).

We have also found that it is practical to transform bacteria cells with a plasmid that codes for the green fluorescence protein (Lower *et al.*, 2000, 2001b). Expression of this protein provides an intracellular "dye," allowing one to visualize the location and orientation of bacteria without the need for stains that kill and/or alter the outer surface of cells (see Fig. 4).

B. Examples of Force Measurements

1. *Where to Begin*

A novice to force microscopy should begin by measuring forces between a clean glass bead (attached to a cantilever) and a clean glass surface or a freshly cleaved piece of mica in air. The most notable force-curve feature will be a large adhesion force in the retraction curve. This adhesion is due to attractive, capillary forces that exist because the surfaces are covered with a layer of water at ambient room humidity. If the humidity is reduced by surrounding the AFM with nitrogen gas, for example, the adhesion force will decrease. Cantilevers of different stiffness should be used so that one can see how a cantilever's spring constant impacts the jump-from-contact feature (see Fig. 3) in the retraction curve.

After force measurements are made in ambient air, the same glass-on-glass (or glass-on-mica) measurement should be performed in aqueous solution. If the surfaces are cleaned properly, the adhesion force should

disappear from the retraction curves when the surfaces are completely submerged in fluid (capillary forces absent). The approach and retraction curves will then plot on top of one another, and they will exhibit a repulsive force of interaction. This repulsive force is due primarily to electrostatic forces, which are sensitive to the ionic strength of the intervening solution (Table I; see Eq. 1). A long-range (~100 nm) repulsive force will likely be observed in low–ionic-strength water (10^{-5} M NaCl); this force will become short range (~1 nm) in 0.1 M NaCl solution. One can experiment with a probe's sensitivity toward these forces by using cantilevers with different spring constants. The size of the bead will also have an impact on the magnitude of the measured forces (see Eq. 1). For the beginner, these approach measurements are important because they can be compared to the first AFM experiments, which were performed with a glass-bead probe on a silicon wafer in saline solution of different ionic strength (Ducker *et al.*, 1991, 1992).

Adhesion forces may be detected between a glass bead and glass cover slip if the surfaces were not cleaned prior to use and/or if epoxy contaminated the surface of the bead (see Fig. 3). While such coatings may be undesirable, they can be used in preliminary force studies for educational proposes. The amount of force that is used to push two surfaces together changes the contact area, which in turn impacts the number of adhesive bonds that may form between two surfaces. While such a scenario may not be of concern for hard surfaces that do not deform (e.g., glass), it is something to consider for soft biological specimens. The greater the length of the region of contact (see Fig. 3) for a particular force curve, the more likely it is there will be a stronger adhesion between a cell and another surface. To normalize this effect for a given experiment, all force curves should be collected with the same "loading force"; otherwise, it is not possible to compare one experiment to another. This is best accomplished by using relative or absolute triggers in the on-line software. The amount of force used to push together two surfaces should be selected so that it has a direct analogy to loading forces that are experienced by bacteria in a natural setting (Lower *et al.*, 2000, 2001b).

After becoming familiar with glass-on-glass measurements, one can use a colloidal glass bead to probe bacteria attached to a cover slip in saline solution. With respect to the actual measurement, the procedure is similar to that for the glass-glass measurement. However, sample preparation will require more effort and care.

Samples should be prepared, at least initially, by adsorbing a monolayer of cells onto a glass cover slip. Obviously, not all bacterial strains will adhere to glass cover slips right out of the box. The "stickiness" of

unclean glass cover slips can vary widely, since every company uses its own proprietary coating and/or manufacturing process. Therefore, one may need to coat the glass cover slip with a positively charged linker (e.g., amino-silane) or a hydrophobic substance such as octadecyltrichlorosilane (Lower *et al.*, 2005). As an example of silane chemistry, we will discuss a procedure for creating a hydrophobic self-assembling layer on glass.

Glass cover slips must first be cleaned overnight in piranha solution (as described previously). Slides should then be rinsed in ultrapure water (18.2 MΩ cm), soaked in a fresh piranha solution for a second night, rinsed ten times in ultrapure water, and finally dried using a stream of pre-purified nitrogen gas. The hydrophobic coating is formed by soaking the cover slips overnight in a 1% solution (by volume) of octadecyltrichlorosilane (in 250 mL toluene with 0.5 mL butylamine). The cover slips should be rinsed in toluene three times and dried with nitrogen gas. If successful, a drop of water will form a steeply sided bead on the surface of the treated glass.

Regardless of how cells are attached to the cover slip, one should ensure that the cells remain viable. There are a variety of fluorescent probes (e.g., LIVE/DEAD BacLight stain from Molecular Probes) that can be used to verify the integrity of a cell wall. Alternatively, cell viability can be assessed by simply placing a drop of broth on the cell-coated cover slip and using a microscope to observe cell division.

2. *Force Measurements Between a Living Bacterium and Material Surface*

This article will conclude by presenting two examples of AFM force measurements for a bacterium and material substrate in aqueous solution. The first example will present forces detected as a bacterium approaches a material surface. The second example will discuss forces detected as a bacterium is pulled away from a material surface. In some instances, the approach and retraction forces are identical. However, in many instances, as is shown in the following events, the approach and retraction force profiles are quite different.

These particular force measurements involve a glass bead (~10 μm diameter) mounted on the end of an AFM cantilever and a wild-type strain of a gram-positive *Staphylococci* in a 0.1 M saline (NaCl) solution at circumneutral pH. The glass bead was cleaned and mounted on an AFM cantilever as described previously. *Staphylococcus* cells were cultured to exponential phase in tryptic soy broth, washed three times in saline solution, and placed on a glass cover slip. Figure 1 (right image) is an atomic force micrograph (collected with a clean silicon

nitride tip) showing the *Staphylococcus* cells used in the experiments. The lateral density of cells within the monolayer was controlled by simply varying the density of cells in the suspension and/or by varying the degree of rinsing of the substrate. This control over cell density allows one to measure forces on a single bacterium or on a cluster of cells.

a. *Forces Detected as a Bacterium Approaches a Material Surface.* Figure 5 shows forces detected as a glass bead is brought into contact with a single cell or binary fission pair of *Staphylococcus*. Shown are 10–15 approach curves chosen at random from a total of ~500 curves collected for three different glass beads and three different cultures of the same strain of *Staphylococcus,* all harvested at precisely the same absorbance. This figure reveals that the bead's surface must approach to within 30 nm of the *Staphylococcus* cell before a measurable force is detected. As the distance between the cell and glass decreases, the bacterium experiences a repulsive force (positive sign) that appears to increase exponentially until the cell and glass make contact (i.e., distance of zero).

Theoretical force-distance expressions can be used to interpret the observed force data. As mentioned in the Introduction (see Table I), there are a few fundamental forces that may exist between surfaces in

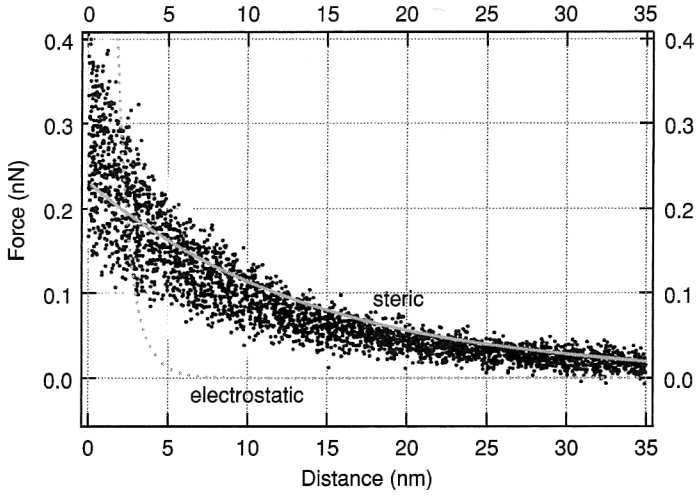

FIG. 5. Forces measured as a glass bead approaches a wild-type strain of *Staphylococcus* in saline solution (0.1M NaCl, circumneutral pH). Each series of dots corresponds to one approach curve. Positive force values indicate repulsion. Gray lines correspond to theoretical electrostatic (dotted) and steric (solid) forces between the glass bead and bacterial cell (or binary fission pair).

aqueous solution. One of these force types is the electrostatic force. A common mathematical expression for the electrostatic force is given as (Elimelech *et al.*, 1995):

$$F(D) = \frac{2\pi r_1 r_2 \varepsilon \varepsilon_0 \kappa}{r_1 + r_2} \left(\frac{k_B T}{z e_c}\right)^2 \frac{\phi_1^2 + \phi_2^2 + (2e^{D\kappa}\phi_1\phi_2)}{(e^{D\kappa} - 1)(e^{D\kappa} + 1)} \quad (1)$$

where F = force (N); D = distance (m); r = radius of the cell or bead, ε is the dielectric constant of water (78.54 at 298 K), ε_0 is the permittivity of free space (8.854×10^{-12} C^2 $J^{-1}m^{-1}$), k_B is Boltzmann's constant (1.381×10^{-23} J K^{-1}), T is temperature (298 K), z is the valence of electrolyte ions (1 for NaCl), and e_c is the charge of an electron (1.602×10^{-19} C). The inverse Debye length (κ, in m^{-1}) describes the thickness of the electrostatic double layer of counter-ions that surrounds charged particles (glass bead or bacterium) in solution. For monovalent electrolytes (e.g., NaCl) at 298 K, the Debye length (κ^{-1}, in nm) is given by $0.304/(c)^{-1/2}$, where c is the concentration of the electrolyte (mol L^{-1}). The final parameter is the surface potential (ϕ) described as [(zeψ)/(kT)], where ψ is the surface potential of the cell or glass bead (in V) and all other parameters are as previously described.

For an aqueous solution at circumneutral pH and ionic strength ~0.1 M, the surface potentials of a glass bead and *Staphylococcus* cell are, respectively, −35 mV (Ducker *et al.*, 1992) and −6 mV (Prince and Dickinson, 2003). Using these values in Equation 1 results in a theoretical expression of the electrostatic force between a *Staphylococcus* bacterium and a glass bead. This theoretical force-distance relationship is shown in Fig. 5.

The electrostatic force is expected to be repulsive and short-range (<5 nm) in a 0.1 M saline solution. While the observed interaction is repulsive, the measured forces are clearly longer-range than expected based solely on electrostatic interactions. Therefore, another of the force types shown in Table I must be involved in the way in which this particular bacterium interacts with the surface of glass.

Staphylococcus cells, like all bacteria, have a surface that is studded with biological polymers. One of the most common biopolymers on *Staphylococcus* is β-1,6-linked glucosaminoglycan, also know as the polysaccharide intercellular adhesin (PIA) (Cramton *et al.*, 1999; Heilmann *et al.*, 1996; Ziebuhr *et al.*, 1997). Polymers such as these emit a steric force of repulsion when they are confined to a narrow space (Israelachvili, 1992; Israelachvili and McGuiggan, 1988). This repulsion is driven by a decrease in entropy that occurs when a polymer is no longer free to move at random. Polymers that are free to move and

rotate in random orientations within a solution are in a higher state of disorder relative to the same polymer that has been confined to a smaller volume of space. This is precisely what occurs when a polymer on a bacterium is confined to a narrowing interface created by an approaching surface (e.g., a glass bead).

Like the electrostatic force (see Eq. 1), the steric force (F) has been described as a function of the distance (D) between two surfaces. This expression, known as the modified Alexander-de Gennes equation, is given by (Butt *et al.*, 1999):

$$F(D) = 50rk_BTL_0\Gamma^{3/2}e^{-2\pi D/L_0} \quad (2)$$

where r = radius of the cell, k_B is Boltzmann's constant (1.381×10^{-23} J K^{-1}), T is temperature (298 K), L_0 is the equilibrium thickness of a polymer (in m) on the cell surface, Γ is the surface density of that same polymer on the cell surface (in m^2).

According to Mack *et al.* (1996), some species of *Staphylococcus* have PIA molecules composed of at least 130 sugar residues. This corresponds to a value for L_0 of ~90 nm (assuming 0.7 nm per glucose residue). While not measured directly, the surface density (Γ) of PIA on a *Staphylococci* cell can be estimated from the work of Mack *et al.* (1996) and Madigan *et al.* (2003). Using these references, we estimate an average value of 4300 PIA polysaccharides per bacterium. For a 2 μm bacterium (i.e., proxy for a fission pair of *Staphylococci* cells), this is equivalent to approximately 3.4×10^{14} PIA per m^2. Using these values for L_0 and Γ in Equation 2 results in a theoretical expression of the steric force between a *Staphylococcus* cell and a glass bead (see Fig. 5).

Comparing the measured forces to the theoretical models reveals that steric forces and electrostatic forces dominate the interactions between *Staphylococcus* and a glass surface in saline solution. The glass substrate must be within 30 nm of the bacterium surface before the forces between the two are measurable (above noise). Steric forces then cause the bacterium to be repelled until the cell is within ~5 nm of the glass. At this close distance, repulsive, electrostatic forces begin to impact the final approach. However, this is only half of the story. We have yet to discuss the forces that were detected while pulling the glass bead from contact with *Staphylococcus*.

b. *Forces Detected as a Bacterium is Pulled From Contact with a Material Surface.* The above force measurements suggest that *Staphylococcus* never forms an attractive bond with glass, because apparently only repulsive forces exist at the bacterium-material interface. However,

it is common knowledge that *Staphylococci* readily adhere to glass slides and cover slips. This apparent discrepancy can be resolved by considering the forces between the glass and bacterium upon retraction of the bead after a period of "forced" contact. The preceding discussion focuses solely on forces observed as a cell approaches another surface. Once contact is established, attractive bonds may form between cell surface macromolecules and reactive sites on a material surface.

Figure 6 shows some retraction curves observed as a glass bead was pulled from a *Staphylococcus* cell after making contact with the bacterium. These data are complementary to the force data shown in Fig. 5. That is, each force measurement consists of an approach curve and a retraction curve, which are collected sequentially during a period of time ranging from a fraction of a second to a few seconds. It is important to note that the retraction data shown in Fig. 6 are curves selected at random from only those measurements that detected an attractive, adhesion force. Not all retraction curves exhibited an adhesive interaction. In many instances, the retraction curve overlaid the approach curves like those shown in Fig. 5.

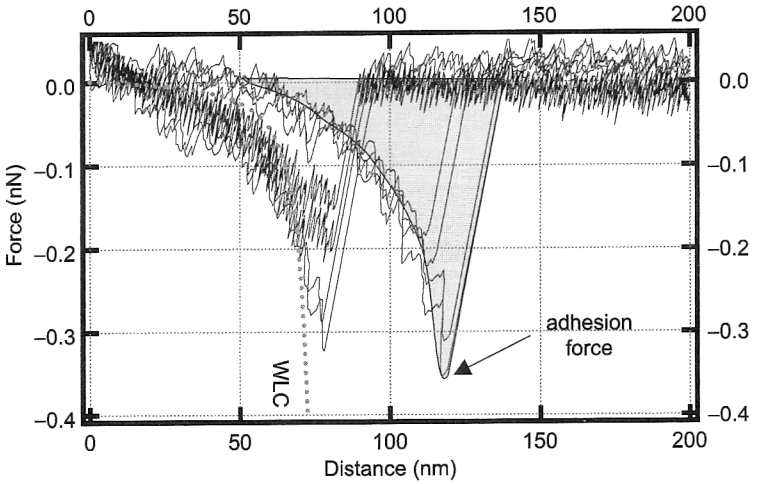

FIG. 6. Forces measured as a glass bead is pulled from contact with the surface of a *Staphylococcus* cell. Five different retraction curves are shown. The attractive forces can be summarized by determining the adhesion force for each curve (0.2–0.35 nN for these data) and/or integrating force with respect to distance (i.e., determining work or energy; see shaded region for two curves). These particular curves exhibit a sawtooth shape indicative of a nonlinear force consistent with the unfolding of a protein that formed a bond with the glass. The dotted line represents the extension profile predicted by the wormlike chain (WLC) model.

At first glance, it is clear that the retraction curves are more complicated than the approach curves. Before exploring the intricate details of these retraction curves, we will describe the overall characteristics of each retraction curve. Each retraction curve can be represented by two parameters: the adhesion force and the work (or energy) necessary to separate a cell from another surface (see Fig. 6). The adhesion force is simply the maximum force detected in a particular retraction curve. As such, this represents a single datum point. The work of adhesion/separation is determined by integrating force with respect to distance (i.e., calculating the area "above" a curve). Therefore, the work calculation embodies the entire retraction curve. We will discuss the adhesion force as an example of how one of these parameters can be used to obtain a general sense of processes occurring at the bacterium-material interface.

More than 500 retraction curves were collected using three different glass-bead cantilevers on 15–20 different *Staphylococcus* cells from three different cultures harvested at precisely the same absorbance. The adhesion force was determined for each of the retraction curves. Figure 7 presents histograms of the maximum adhesion force recorded

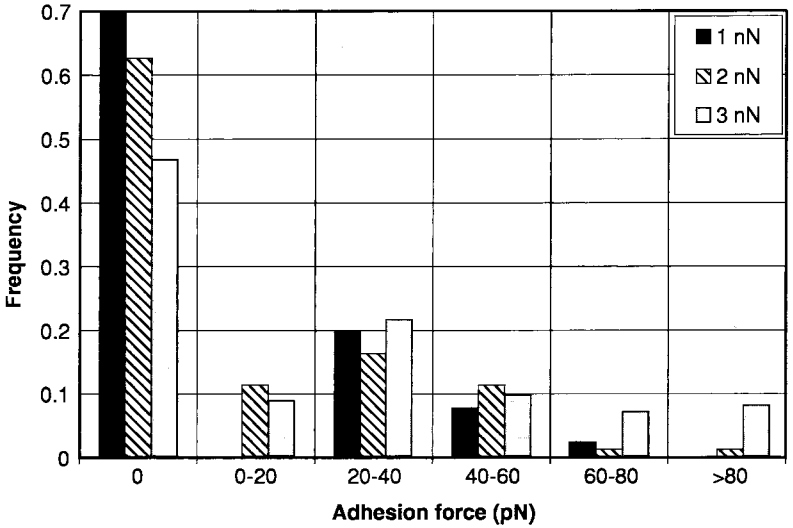

FIG. 7. Histograms of the adhesion force recorded in retraction curves like those shown in Fig. 6. Note that adhesion forces are in picoNewtons (10^{-12} N). The loading force placed on a cell is given as 1, 2, or 3 nN. An adhesion force of zero means that no attractive force was detected in a retraction curve (i.e., both the approach and retraction curves looked like the curves presented in Fig. 5).

as the glass bead was pulled away from a cell. While taking these measurements, we varied the "loading force," or force with which the bead was pressed against a bacterium. This loading force, which is controlled by using "triggers" (software-specific controls) during force measurements, ranged from 1 to 3 nN.

The histograms show a correlation between the loading force and the frequency of adhesion. An attractive bond was 10–25% more likely to form at a loading force of 3 nN relative to 1 or 2 nN. This is probably due to the increased contact area created when the bead was pushed against the cell wall of the bacterium. This highlights the fact that it is important to carefully control and/or measure the loading force (and loading rate) placed on a bacterium by a cantilever probe.

Summary data like that shown in Fig. 7 are valuable, but they do not address the intricacies of individual retraction curves. Retraction curves like those shown in Fig. 6 contain a unique force profile that looks like a tooth on a saw, a so-called sawtooth. These sawtooth force signatures are regions where there is a strong, nonlinear increase in the attractive force that suddenly snaps back toward the line of zero force at increasing separation distance. Within a single retraction curve, sawteeth may occur as single or multiple events that extend outward for hundreds of nanometers.

Recently, we showed that sawtooth features in retraction profiles originate because biological polymers (e.g., proteins) form a specific bond between a cell and another surface (Lower *et al.*, 2005). The force-extension profile of a linear polymer that forms a bridging bond between a cell and another surface can be modeled with the worm-like chain theory (Flory, 1989). This theory predicts a highly nonlinear relationship between force (F) and distance (D) as a linear polymer (e.g., a polypeptide) is extended in solution. The worm-like chain model is given by:

$$F(x) = (k_B T/b)[0.25(1 - D/L)^{-2} + D/L - 0.25] \quad (3)$$

where k_B is Boltzmann's constant (1.381×10^{-23} J K^{-1}), T is temperature (298 K), L is the contour length or overall length of a polymer (in m), and b is the persistence length of the polymer. Each biological polymer (e.g., protein, nucleic acid, polysaccharide) has its own intrinsic persistence length. For proteins, the persistence length has been determined to be the length scale of a single amino acid (~0.1 to 0.4 nm; Mueller *et al.*, 1999; Oberhauser *et al.*, 1999). By applying this equation to retraction profiles, one can determine whether a protein, for example, might be responsible for a particular sawtooth force-signature

(see WLC curve in Fig. 6). Of course, any linear polymer (e.g., proteins, some polysaccharides or extracellular nucleic acid) that forms a bond between a cell and substrate might also display a sawtooth-like force profile in a retraction curve. Assignment of a particular force signature to a specific cell wall biomolecule is possible if one uses bacterial mutants that cannot produce a particular cell wall macromolecule and/or enzymes (e.g., proteases) that will degrade a polymer of interest. For example, one can compare retraction curves from a wild-type strain and a mutant strain that cannot produce a specific cell wall polymer (Lower *et al.*, 2005).

V. Conclusions

AFM force measurements can investigate aspects of bacteria-surface interactions inaccessible to more traditional microbiology techniques, such as optical microscopy or batch culture experiments. Approach of the AFM probe into contact with a bacterium allows the creation of a bacteria-surface interface. Subsequent retraction of the probe allows a view into the specific dynamic interactions that create and maintain the interface. A great deal of care and perseverance are required to extract valid and meaningful conclusions from the force measurements. In spite of the difficulties involved, there is no doubt that AFM experiments will continue to greatly enhance our understanding of the nature of bacteria-surface interactions.

Acknowledgments

This work was supported by grants from the Department of Energy, the National Science Foundation, and the American Chemical Society. We also thank F. Paul Vellano III for his help with culturing and preparing cells for AFM measurements. RY and SKL acknowledge the encouragement and support of CSY and J. Tak, respectively.

References

Albrecht, T. R., Akamine, S., Carver, T. E., and Quate, C. F. (1990). Microfabrication of cantilever styli for the atomic force microscope. *J. Vac. Sci. Technol. A: Vac. Surf. Films* **8,** 3386–3396.

Binnig, G., Quate, C. F., and Gerber, C. (1986). Atomic force microscope. *Phys. Rev. Lett.* **56**(9), 930–933.

Boland, T., and Ratner, B. D. (1995). Direct measurement of hydrogen bonding in DNA nucleotide bases by atomic force microscopy. *Proc. Nat. Acad. Sci. USA* **92,** 5297–5301.

Bowen, W. R., Lovitt, R. W., and Wright, C. J. (2000). Direct quantification of *Aspergillus niger* spore adhesion in liquid using an atomic force microscope. *J. Colloid Interface Sci.* **228**(2), 428–433.

Butt, H. J., Jaschke, M., and Ducker, W. (1995). Measuring surface forces in aqueous electrolyte solution with the atomic force microscope. *Bioelectrochem. Bioenerg.* **38,** 191–201.

Butt, H. J., Kappl, M., Mueller, H., Raiteri, R., Meyer, W., and Ruhe, J. (1999). Steric forces measured with the atomic force microscope at various temperatures. *Langmuir* **15**(7), 2559–2565.

Cappella, B., and Dietler, G. (1999). Force-distance curves by atomic force microscopy. *Surf. Sci. Rep.* **34,** 1–104.

Cleveland, J. P., Manne, S., Bocek, D., and Hansma, P. K. (1993). A nondestructive method for determining the spring constant of cantilevers for scanning force microscopy. *Rev. Sci. Instrum.* **64,** 403–405.

Craig, V. S. J., and Neto, C. (2001). *In situ* calibration of colloid probe cantilevers in force microscopy: Hydrodynamic drag on a sphere approaching a wall. *Langmuir* **17**(19), 6018–6022.

Cramton, S. E., Gerke, C., Schnell, N. F., Nichols, W. W., and Gotz, F. (1999). The intercellular adhesion (ica) locus is present in *Staphylococcus aureus* and is required for biofilm formation. *Infection and Immunity* **67**(10), 5427–5433.

Dammer, U., Popescu, O., Wagner, P., Anselmetti, D., Guntherodt, H. J., and Misevic, G. N. (1995). Binding strength between cell adhesion proteoglycans measured by atomic force microscopy. *Science* **267,** 1173–1175.

D'Costa, N. P., and Hoh, J. H. (1995). Calibration of optical lever sensitivity for atomic force microscopy. *Rev. Sci. Inst.* **66,** 5096–5097.

Ducker, W. A., Senden, T. J., and Pashley, R. M. (1991). Direct measurement of colloidal forces using an atomic force microscope. *Nature* **353,** 239–241.

Ducker, W. A., Senden, T. J., and Pashley, R. M. (1992). Measurements of forces in liquids using a force microscope. *Langmuir* **8,** 1831–1836.

Elimelech, M., Gregory, J., Jia, X., and Williams, R. (1995). Particle Deposition & Aggregation: Measurement, Modeling, and Simulation. Butterworth-Heinemann.

Florin, E. -L., Moy, V. T., and Gaub, H. E. (1994). Adhesion forces between individual ligand-receptor pairs. *Science* **264,** 415–417.

Flory, P. J. (1989). Statistical Mechanics of Chain Molecules. Hanser Publishers.

Frank, B. P., and Belfort, G. (1997). Intermolecular forces between extracellular polysaccharides measured using the atomic force microscope. *Langmuir* **13,** 6234–6240.

Heilmann, C., Schweitzer, O., Gerke, C., Vanittanakom, N., Mack, D., and Gotz, F. (1996). Molecular basis of intercellular adhesion in the biofilm-forming *Staphylococcus epidermidis*. *Mol. Microbiol.* **20**(5), 1083–1091.

Hinterdorfer, P., Baumgartner, W., Gruber, H. J., Schilcher, K., and Schindler, H. (1996). Detection and localization of individual antibody-antigen recognition events by atomic force microscopy. *Proc. Nat. Acad. Sci. USA* **93,** 3477–3481.

Hutter, J. L., and Bechhoefer, J. (1993). Calibration of atomic-force microscope tips. *Rev. Sci. Inst.* **64,** 1868–1873.

Israelachvili, J. (1992). Intermolecular and Surface Forces. Academic Press.

Israelachvili, J. N., and McGuiggan, P. M. (1988). Forces between surfaces in liquids. *Science* **241,** 795–800.

Kendall, T. A., and Lower, S. K. (2004). Forces between minerals and biological surfaces in aqueous solution. *Adv. Agron.* **82,** 1–54.

Leckband, D., and Israelachvili, J. (2001). Intermolecular forces in biology. *Quarterly Rev. Biophys.* **34**(2), 105–267.

Lee, G. U., Chrisey, L. A., and Colton, R. J. (1994). Direct measurement of the forces between complementary strands of DNA. *Science* **266,** 771–773.

Lo, Y. S., Huefner, N. D., Chan, W. S., Dryden, P., Hagenhoff, B., and Beebe, T. P., Jr (1999). Organic and inorganic contamination on commercial AFM cantilevers. *Langmuir* **15**(19), 6522–6526.

Lower, B. H., Yongsunthon, R., Vellano, F. P., and Lower, S. K. (2005). Simultaneous force and fluorescence measurements of a protein that forms a bond between a living bacterium and a solid surface. *J. Bacteriol.* **187**(6), 2127–2137.

Lower, S. K. (2005). Directed forces of affinity between a bacterium and mineral. *Am. J. Sci.* In press.

Lower, S. K., Hochella, M. F., and Beveridge, T. J. (2001a). Bacterial recognition of mineral surfaces: Nanoscale interactions between *Shewanella* and α-FeOOH. *Science* **292**(5520), 1360–1363.

Lower, S. K., Tadanier, C. J., and Hochella, M. F. (2000). Measuring interfacial and adhesion forces between bacteria and mineral surfaces with biological force microscopy. *Geochimica et Cosmochimica Acta* **64**(18), 3133–3139.

Lower, S. K., Tadanier, C. J., and Hochella, M. F. (2001). Dynamics of the mineral-microbe interface: Use of biological force microscopy in biogeochemistry and geomicrobiology. *Geomicrobiol. J.* **18**(1), 63–76.

Mack, D., Fischer, W., Krokotsch, A., Leopold, K., Hartmann, R., Egge, H., and Laufs, R. (1996). The intercellular adhesin involved in biofilm accumulation of *Staphylococcus epidermidis* is a linear beta-1, 6-linked glucosaminoglycan: Purification and structural analysis. *J. Bacteriol.* **178**(1), 175–183.

Madigan, M. T., Martinko, J. M., and Parker, J. (2003). Brock Biology of Microorganisms. Prentice Hall.

Moy, V. T., Florin, E.-L., and Gaub, H. E. (1994). Adhesion forces between ligand and receptor measured by AFM. *Colloids and Surfaces A: Physicochemical and Engineering Aspects* **93**, 343–348.

Moy, V. T., Florin, E.-L., and Gaub, H. E. (1994). Intermolecular forces and energies between ligands and receptors. *Science* **266**, 257–259.

Mueller, H., Butt, H. J., and Bamberg, E. (1999). Force measurements on myelin basic protein adsorbed to mica and lipid bilayer surfaces done with the atomic force microscope. *Biophys. J.* **76**, 1072–1079.

Muller, D. J., Baumeister, W., and Engel, A. (1999). Controlled unzipping of a bacterial surface layer with atomic force microscopy. *Proc. Nat. Acad. Sci. USA* **96**(23), 13170–13174.

Oberhauser, A. F., Marszalek, P. E., Carrion-Vazquez, M., and Fernandez, J. M. (1999). Single protein misfolding events captured by atomic force microscopy. *Nat. Struc. Biol.* **6**(11), 1025–1028.

Parsek, M. R., and Fuqua, C. (2004). Biofilms 2003: Emerging themes and challenges in studies of surface-associated microbial life. *J. Bacteriol.* **186**(14), 4427–4440.

Pincet, F., Perez, E., and Wolfe, J. (1995). Does glue contaminate the surface forces apparatus? *Langmuir* **11**, 373–374.

Pleuddemann, E. P. (1991). Silane Coupling Agents. Plenum Press.

Prince, J. L., and Dickinson, R. B. (2003). Kinetics and forces of adhesion for a pair of capsular/unencapsulated *Staphylococcus* mutant strains. *Langmuir* **19**(1), 154–159.

Razatos, A., Ong, Y.-L., Sharma, M. M., and Georgiou, G. (1998). Molecular determinants of bacterial adhesion monitored by atomic force microscopy. *Proc. Nat. Acad. Sci. USA* **95**, 11059–11064.

Sader, J. E. (1995). Parallel beam approximation for V-shaped atomic force microscope cantilevers. *Rev. Sci. Inst.* **66**, 4583–4587.

Senden, T. J., and Ducker, W. A. (1994). Experimental determination of spring constants in atomic force microscopy. *Langmuir* **10,** 1003–1004.

Tortonese, M. (1997). Cantilevers and tips for atomic force microscopy. *IEEE Eng. Med. Biol.* **16,** 28–33.

Watnick, P., and Kolter, R. (2000). Biofilm, city of microbes. *J. Bacteriol.* **182**(10), 2675–2679.

Whitman, W. B., Coleman, D. C., and Wiebe, W. J. (1998). Prokaryotes: The unseen majority. *Proc. Nat. Acad. Sci. USA* **95**(12), 6578–6583.

Willemsen, O. H., Snel, M. M. E., Kuipers, L., Figdor, C. G., Greve, J., and De Grooth, B. G. (1999). A physical approach to reduce nonspecific adhesion in molecular recognition atomic force microscopy. *Biophys. J.* **76**(2), 716–724.

Ziebuhr, W., Heilmann, C., Gotz, F., Meyer, P., Wilms, K., Straube, B., and Hacker, J. (1997). Detection of the intercellular adhesion gene cluster (ica) and phase variation in *Staphylococcus epidermidis* blood culture strains and mucosal isolates. *Infection and Immunity* **65**(3), 890–896.